

## INHOMOGENEOUS STRAINS IN SMALL PARTICLES

L.D. MARKS

*Department of Physics, Arizona State University, Tempe, Arizona 85287, USA*

Received 12 July 1984; accepted for publication 23 October 1984

This paper considers the evidence for strains in small particles. Firstly, the dynamical electron diffraction theory for dark field imaging of small particles is briefly reviewed, considering primarily the effects of strain on wedge crystals and identifying the fingerprint of strain contrast effects under strong beam conditions. Evidence included herein and from published papers by other authors clearly shows inhomogeneous strain effects in both multiply twinned particles and single crystals. Considering these results and earlier reports of lattice parameter changes, there are problems with the uniqueness of these analyses, and the strains in the small single crystals are thought more likely to be due to interfacial stresses or contaminants than any intrinsic particle effect; there are so many different origins of this type of strain that we cannot with confidence isolate a unique source. It is emphasised that the uniqueness of any interpretation of experimental results from small particles must be very carefully considered.

### 1. Introduction

The question of lattice strains and/or lattice parameter changes in small metal particles has been a subject of some debate for many years. Three essential sources can be identified, namely interfacial stress (e.g. ref. [1]), intrinsic lattice parameter changes (e.g. refs. [2,3]), or a morphological change (e.g. ref. [4]). To these should be added effects which can lead to apparent changes (when averaged over a particle), namely surface relaxations (e.g. ref. [5]) or (anharmonic) surface vibrations (e.g. ref [6]). The question, although academic in many ways, includes some important physics: are small particles structurally fundamentally different, a “fifth state of matter”, or simply bridges between atoms and solids?

One particular problem has been the structure of the non-crystallographic particles called multiply-twinned particles or MTPs [7–35]. Following the original model of Ino [7] and Ino and Ogawa [8] which just preempted the work of Allpress and Sanders [9], these are derived from an fcc structure by an inhomogeneous strain which is compensated for by a favorable surface energy. The alternative view that originated with Bagley [10] and has been pursued by Schabes-Retchkiman et al. [11,12] and Yacaman [13] is that these particles are

not fcc, but have orthorhombic or rhombic crystallographies. This assumes that there is a Jahn–Teller or Peierls distortion in the particles. Both homogeneous [10–17] and inhomogeneous (e.g. refs. [7–9,18–30]) models have had their proponents, the weight of evidence being substantially in favor of inhomogeneous strains. The uniqueness of the evidence for homogeneous strains has previously been questioned [26,29], and further comments can be found in the discussion in section 4. The larger multiply-twinned particles certainly contain inhomogeneous strains as evidenced by the formation of dislocations in the icosahedral particles [25–27,29–30] and stacking faults in the decahedral particles [19,25–27,29–30], these defect structures correlating with inhomogeneous elasticity calculations [30].

In this paper we look carefully at the evidence for inhomogeneous strains in small gold particles using dark field electron microscopy. Section 2 is a brief review of the dynamical analysis for strained wedge crystals where we point out that strong beam and *not* weak beam is the correct technique for identifying strains. This section has been included since the signature of strain in a small particle is different to that encountered in electron microscopy of continuous thin films. For the latter, the thickness is generally constant and inhomogeneous strains are indicated by amplitude changes. In a small particle the thickness is rapidly varying, and this complicates the problem. It is necessary to consider the intensity along a contour where the intensity is maximised. If this maximum intensity varies, inhomogeneous strains are present. In section 3 we consider the experimental evidence, concluding that not only from the results shown here, but also from essentially *every* published paper, that inhomogeneous strains are present both in MTPs and in single crystals. Finally, in the discussion we consider the interpretation of the strains in the small single crystal particles, considering carefully the uniqueness of the data, and concluding that lattice parameter changes and trace inhomogeneous strains are probably a result of interfacial stresses with the support film or other surface contaminants. We also emphasise the importance of checking the uniqueness of any interpretation of experimental data.

## 2. Diffraction theory

The basis within which dynamical electron diffraction is discussed analytically is the Bloch Wave formalism (e.g. refs. [36–41]). A dynamical, rather than a kinematical analysis is the only correct approach for high energy electrons because the elastic scattering is so strong – the standard benchmark is that at 100 keV, one atom of gold is a dynamical scatterer. For convenience we will employ the non-relativistic wave equations, which should contain relativistically corrected rest-masses and wavelengths.

Considering Schrödinger's equation for the electrons in the form

$$\{ \nabla^2 + (8\pi^2 me/h^2)[E + V(\mathbf{r})] \} \psi(\mathbf{r}) = 0, \quad (1)$$

where  $V(\mathbf{r})$  is the crystal potential and the remainder of the notation is standard, we look for a series solution based upon Bloch waves  $B_j(\mathbf{k}_j, \mathbf{r})$ , i.e.

$$\psi(\mathbf{r}) = \sum_j A_j(\mathbf{k}_j) B_j(\mathbf{k}_j, \mathbf{r}), \quad (2)$$

$$B_j(\mathbf{k}_j, \mathbf{r}) = \sum_g C_g^j(\mathbf{k}_j) \exp[-2\pi i(\mathbf{k}_j + \mathbf{g}) \cdot \mathbf{r}]. \quad (3)$$

Substituting (2) into eq. (1) with a Fourier expansion of the potential

$$V(\mathbf{r}) = \sum_g V_g \exp(2\pi i \mathbf{g} \cdot \mathbf{r}), \quad (4)$$

we obtain

$$\left[ 1 - (\mathbf{k}_j + \mathbf{g})^2 h^2 / (2meE) \right] C_g^j(\mathbf{k}_j) + (1/E) \sum_h V_h C_{g-h}^j(\mathbf{k}_j) = 0, \quad (5)$$

the standard matrix equation for high energy diffraction. This equation only has solutions for specific values of  $\mathbf{k}_j$ , these being different from each "j" solution for the coefficients  $C_g^j(\mathbf{k}_j)$ . The  $\mathbf{k}_j$  wavevectors are generally considered via a dispersion surface (e.g. refs. [36–41]), essentially the same as the construction used in band structure analysis. (We note that it is conventionally drawn with the "y" axis inverted relative to the solid state usage.) The relationship to band structures is discussed by Stern et al. [42], and a recent description of numerical techniques for solving these equations can be found in the paper by Self et al. [43].

To determine the wavevector and  $A_j(\mathbf{k}_j)$ , the Bloch waves are matched at the specimen entrance surface to (generally) an incoming plane wave. Geometrically, the match is accomplished by projecting from the free electron sphere onto the dispersion surface as illustrated in fig. 1. An analysis of various boundary conditions can be found in the article by Metherell [38]. With a wedge shaped crystal, a similar normal projection is used on the exit surface as also shown in fig. 1. The result is to produce a refractive multiplet of diffracted beams, rather than simply one (e.g. see ref. [44]). The explanation [45] of these effects was one of the early successes of dynamical diffraction, and observations of these effects as a function of orientation (e.g. refs. [46–48]) provided some of the first evidence for the high energy dispersion surface.

There is an important conceptual trap in the dispersion surface construction which we will draw attention to here. (A more detailed analysis can be found in refs. [49,50].) With any wave system, a ray diagram corresponds to the propagation direction of a bundle of waves centered on some wavevector  $\mathbf{k}$ . This propagation direction is *not*  $\mathbf{k}$ , the *phase* velocity, but the *group* velocity

$\nabla_k(k \cdot r)$ . Thus each Bloch wave propagates as an entity through the crystal in the direction  $\nabla_k(k_j \cdot r)$ , and it is *wrong* to consider the different diffracted beams as propagating in the directions  $k_j + g$ . The group velocity lies normal to the dispersion surface, and leads to a refractive index which can be either

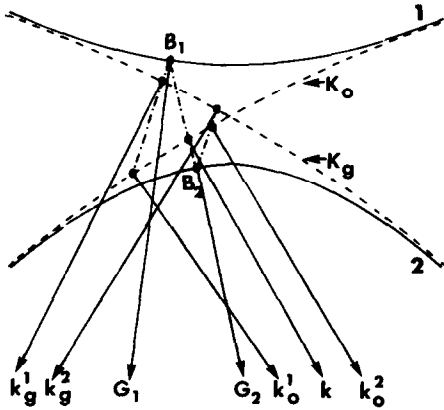


Fig. 1. Dispersion surface construction for a wedge shaped crystal showing two branches labelled 1 and 2, and the free electron spheres for the incident direction ( $K_0$ ) and diffracted beams ( $K_g$ ). Starting with an incident wave  $k$ , points  $B_1$  and  $B_2$  are excited yielding rays propagating along  $G_1$  and  $G_2$  respectively. These match on the exit surface to produce pairs of transmitted ( $k_0^1, k_0^2$ ) and diffracted ( $k_g^1, k_g^2$ ) beams. See also fig. 2.

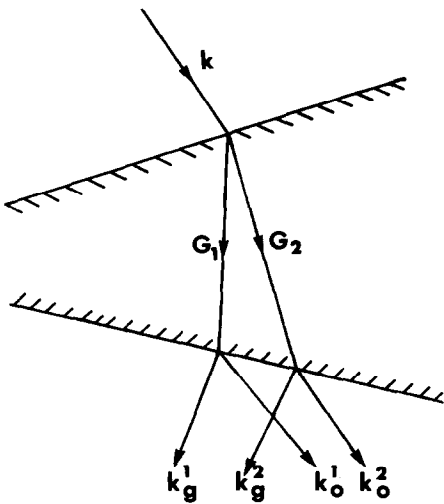


Fig. 2. Real space ray diagram for a wedge shaped crystal, with the notation as in fig. 1.

positive or negative. An analysis of refraction effects in terms of the group velocity can be found in Born and Wolf [51]. For reference, a ray diagram construction for a wedge crystal is shown in fig. 2.

The splitting of each diffracted beam produces, when these beams interfere in the image, a fringe structure called *pendellosung* or thickness fringes. Each contour in the image represents (in the absence of strains) the contour of a particular thickness, the thickness increment being a constant which is inversely proportional to the separation between the dispersion surfaces. Under weak beam conditions (e.g. refs. [37,41,52–54]), the separation between the dispersion surfaces is large, leading to small increments between the thickness contours, about 2 nm in the case of fig. 3. We note that inelastic and phonon scattering will modify the above results for thicknesses substantially larger than those normally encountered in small particles work; for the relatively large particle in fig. 3, the decrease in fringe intensity in the thicker, central region is due to these.

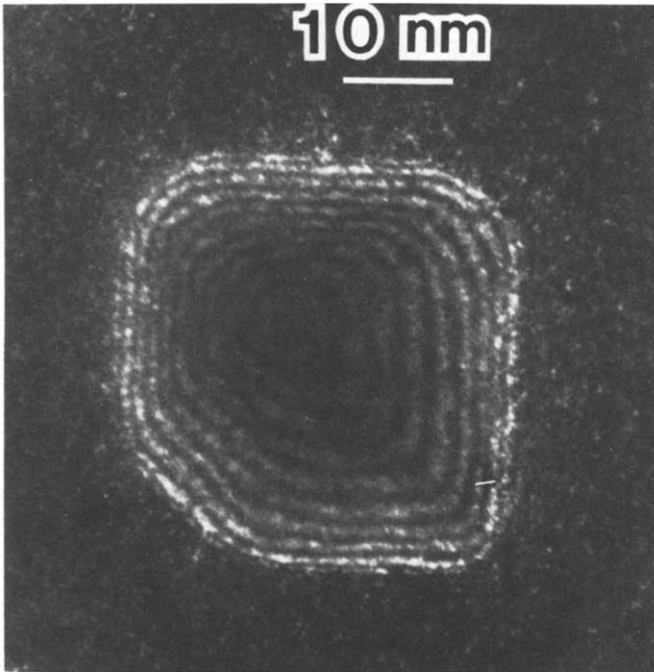


Fig. 3. Weak beam dark field electron micrograph of a single crystal of gold. The intensity contours correspond to equal thickness increments. The particle is square pyramidal with one fairly large additional (110) facet. The speckled background in this and later images is from the amorphous carbon substrate.

When strains are present in the crystal, much of the simple elegance of the Bloch wave formalism is lost. Perhaps the only analytical case is for a constant strain gradient and two beams (e.g. refs. [55–58]). The standard (e.g. refs. [36,38–41]) approach is to follow the formalism of Tagaki [59] and consider the strain as changing the crystal potential:

$$V(\mathbf{r}) \rightarrow V(\mathbf{r} - \mathbf{R}) = \sum_{\mathbf{g}} V_{\mathbf{g}} \exp[2\pi i \mathbf{g} \cdot (\mathbf{r} - \mathbf{R})], \quad (6)$$

where  $\mathbf{R}$  is the elastic displacement field. The main effect of the strain is to introduce a local tilt of the lattice (in radians) of  $2\pi \partial \mathbf{R} / \partial z$ , see for instance refs. [36,39–40]. (There are additional small terms due to lattice rotations normal to the incident beam direction. Experimental evidence that these can be safely neglected can be found in Hashimoto and Mannami [60].) A number of different numerical approaches for analysing strain effects have been used to calculate the contrast from dislocations (see, for instance, ref. [39]). A common approach is to integrate the scattering down to  $z$  direction (e.g. refs. [36,40,61–64]). Alternatively, one may use the multislice approach (e.g. ref. [37]) for a strained crystal (e.g. ref. [65]).

A useful and general result, however, can be obtained without numerical analysis. In a semi-classical picture (essentially WKB) we consider an electron projectile moving along a ray, with the Group velocity the projectile velocity. In the standard, solid-state analysis (e.g. ref. [66]) the effective particle mass is inversely proportional to the curvature of the dispersion surface. As pointed out by Kato [67], the classical analogue of the strain field is an electric field. Now considering the dispersion surface in the region of a two beam orientation (Brillouin zone), as in fig. 1, the dispersion surface curvature is large so that the effective mass is small. Hence there is a strong response to the strain field; the particle is light, so that there is a large response to the electric field. By comparison, in a weak beam orientation the dispersion surface is almost flat so that effective mass is large and the response to strains is small. The relative sensitivity is well known for dislocation imaging – in a two beam orientation the long range dislocation strain field is imaged, whilst in weak beam only the highly distorted core region contributes. We note that since the angles in high energy electron diffraction are so small, trace strains can yield noticeable effects.

So far we have been dealing with the general case where the electron beam inside the crystal is represented by a large number of Bloch waves. Fortunately, for most circumstances in electron microscopy it is only necessary to employ a limited number of Bloch waves, often only two [36]. To further discuss the effects we will therefore make this two beam approximation. This gives for the transmitted  $\phi_0(\mathbf{r})$  and diffracted  $\phi_{\mathbf{g}}(\mathbf{r})$  intensities

$$\phi_0(\mathbf{r}) = \cos(\pi z s_{\mathbf{g}}^{\text{eff}}) - i \cos \beta \sin(\pi z s_{\mathbf{g}}^{\text{eff}}), \quad (7)$$

$$\phi_g(\mathbf{r}) = i \sin \beta \sin(\pi z s_g^{\text{eff}}), \quad (8)$$

where

$$\psi(\mathbf{r}) = [\phi_0 + \phi_g \exp(-2\pi i \mathbf{g} \cdot \mathbf{r})] \exp(-2\pi i \mathbf{k}_0 \cdot \mathbf{r}), \quad (9)$$

$\mathbf{k}_0$  being the incident beam direction,

$$s_g^{\text{eff}} = \sqrt{s^2 + 1/\epsilon_g^2},$$

$$s\epsilon_g = \cot \beta, \quad (10)$$

where  $\epsilon_g$  is the extinction distance (the inverse of the minimum separation between the two branches of the dispersion surface), and  $s$  the effective local excitation error which for a strained crystal is (to first order) the column average off

$$2\pi \lambda \mathbf{g} \cdot \frac{\partial \mathbf{R}}{\partial z} + s_0,$$

$s_0$  being the excitation error for an unstrained crystal.

We should be aware of two approximations in these equations. Firstly, they use a surface which is normal to the incident electron beam, rather than inclined. This corresponds to a vertical fit on the dispersion surface, rather than an inclined matching as described earlier. Geometrically, the error involved in this will be proportional to the separation between the branches and will be larger for weak beam conditions, when the exact fringe periodicity and the oscillation amplitude will become functions of the precise inclination angle of the surface. This effect is small, and can only just be discerned by the change in fringe intensity as a function of face in fig. 3. We note that the detailed calculations by Heinemann et al. [68] missed this effect by implicitly using beam normal boundary conditions.

A second approximation in the two-beam form is that the propagation direction is the incident beam direction, i.e. an approximation for the Group velocity. Strictly one should integrate along the Group velocity directions rather than down a column, ideally using the ray paths for modified Bloch waves as described by Kato [49]. This approximation and the neglect of the higher order dispersive terms which lead to transverse spreading is termed the column approximation. Again, near a strong two-beam orientation the effects are small, but they can be large for a weak beam orientation where the column approximation is known to breakdown (e.g. ref. [39]).

Continuing the analysis, to generate the sense of strain effects, we note that the fringe maximum in dark field ( $\phi_g$  imaged) is

$$I_{\text{max}} = (s^2 \epsilon_g^2 + 1)^{-1}, \quad (11)$$

for

$$z = (n + 1/2)(s^2 + 1/\epsilon_g^2)^{-1/2}, \quad n = 0, 1, \dots \quad (12)$$

Considering strain as (approximately) changing the value of  $s$ , and following the contour of maximum intensity, we find that strain contrast changes this maximum intensity most when  $s = \pm 1/\epsilon_g$ . These two roots correspond to very small tilts on either side of the exact two beam ( $s = 0$ ) orientation. Thus strain will lead to intensity changes along the contour of maximum intensity, these being most pronounced in a strong beam condition. The contours are best termed extinction contours to avoid ascribing a constant thickness to them. The larger the strain, obviously the larger will be the intensity variations. Thus large strains will be evident even in weak beam conditions. We note that we are using strains here implicitly as inhomogeneous (space varying) strains. Homogeneous strains lead to a space invariant lattice change and thus will not result in any contrast variations. Since strains can be described by a Taylor series, there will be a homogeneous component corresponding to the average strain. Experimentally it does not matter how this homogeneous term is described, but theoretically the distinction is important. Ascribing it to anything other than

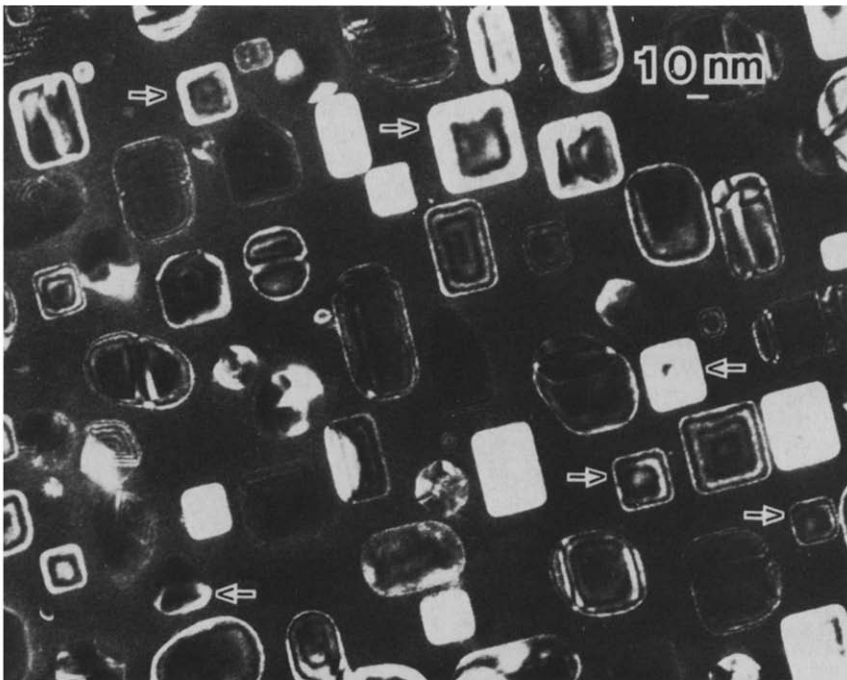


Fig. 4. Dark field micrograph showing a relatively large area. A number of cases of strain contrast (intensity variations along an extinction contour) are arrowed. Note that all the single crystal particles near to a strong beam condition display inhomogeneous strain effects. The presence of strains should not be a surprising result, as discussed later in the text.

the homogeneous component of an inhomogeneous strain implies the existence of a Jahn-Teller or Peierls distortion. At present there does not appear to be any evidence for these in small particles.

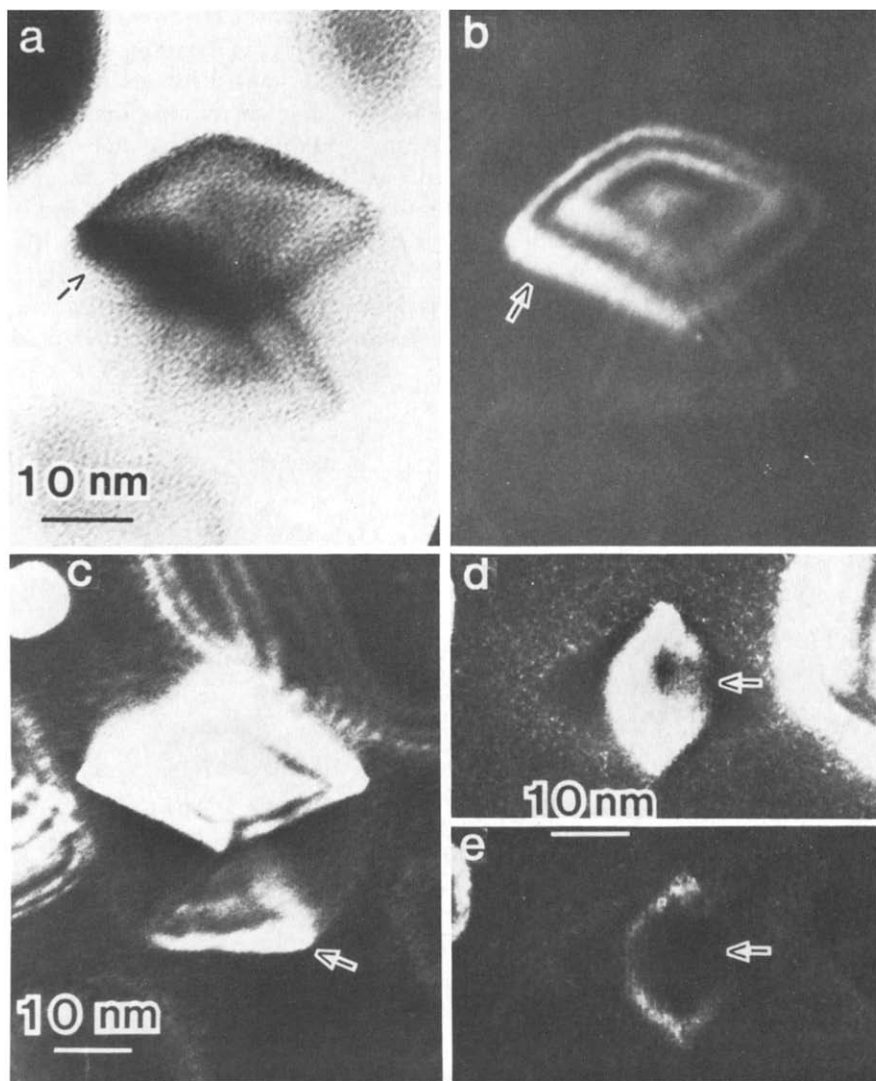


Fig. 5. Micrographs showing strain contrast in decahedral MTPs. In (a) and (b) a bright field/dark field pair for a  $\langle 111 \rangle$  oriented particle. Strain contrast in both bright and dark field images is present, particularly in the area arrowed. In (c), dark field micrograph showing strain contrast (arrowed) in the  $\langle 111 \rangle$  oriented epitaxial segment of a particle. In (d) and (e)  $\pm(200)$  dark field images of a  $\langle 100 \rangle$  epitaxial particle, with strain contrast again arrowed.

### 3. Evidence for strain

With the information that intensity variations along a contour are a strain fingerprint, figs. 4–9 show evidence for inhomogeneous strains in small gold isocahedral MTPs, decahedral MTPs, and single crystals. Descriptions of the results are given in the figure captions. The feature to note is the large intensity variations along the nominal thickness contours, the signature of inhomogeneous strains. Dark field micrographs showing similar strain contrast in small particles can be found in refs. [7–9,12,14–15,23,31–33,68–69]. (The gold particles in figs. 4–9 were prepared by epitaxial vapour deposition as described elsewhere [26].) It is important to compare the images in figs. 9a and 9b which were taken from square pyramidal single crystals. These particles have flat (111) facets which are correctly represented in the weak beam micrograph. (Independent confirmation of the atomic flatness of these surfaces was obtained by direct surface imaging, e.g. refs. [70–72].) In fig. 9b there is enough strain contrast to distort the simple fringe contrast. This indicates that only weak beam conditions (rather than any dark field condition) should be used for three-dimensional particle shape determination. This is a troublesome experimental constraint since it is difficult to controllably tilt a single particle and determine the precise diffracting conditions. We note that the contrast in MTPs is stronger than that in the single crystals, as expected from the relative strain magnitudes [30], and also that the single crystals *as a rule* showed evidence for trace inhomogeneous strains. The observation of strains in the

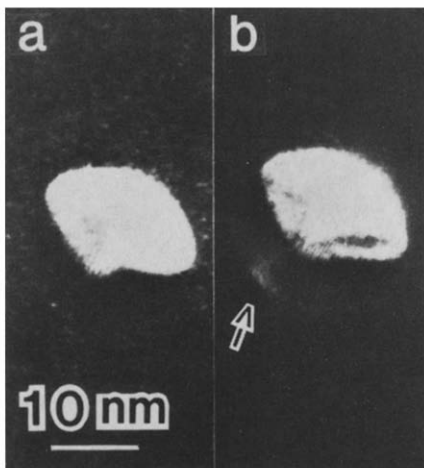


Fig. 6. Pair of  $\pm g$  dark field images including (111) and (220) spots from a small decahedral MTP. The strain contrast (arrowed) demonstrates that the smaller particles are also inhomogeneously strained.

single crystals should be no surprise and can be attributed to either or both tractions at the carbon-gold interface or an intrinsic surface stress (e.g. refs. [2,3]).

#### 4. Discussion

The question now remains as to whether the case for inhomogeneous strains in MTPs is final, and it is important to consider the uniqueness of any experimental results. One of the main results in favor of homogeneous distortions was the observation that many nominally  $\langle 111 \rangle$  oriented segments in

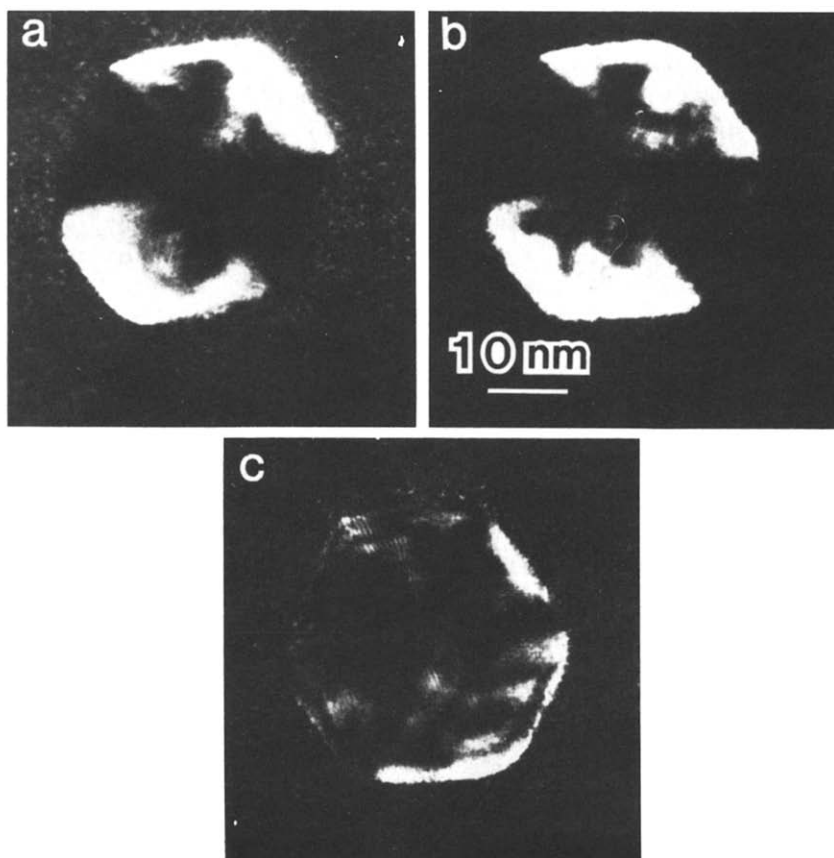


Fig. 7. Trio of dark field images of the same icosohedral MTP using different diffracted beams. There are extensive intensity variations rather than simple thickness fringes (of constant maximum intensity), indicative of the large inhomogeneous strains in these particles.

these particles did not display all six (220) diffraction spots [14–17]. However, this can be attributed to particle rotations [29], the particles not being truly  $\langle 111 \rangle$  oriented. Furthermore, fig. 4 in ref. [80] unambiguously contradicts this evidence. We should also point out that particle rotations, evidenced by

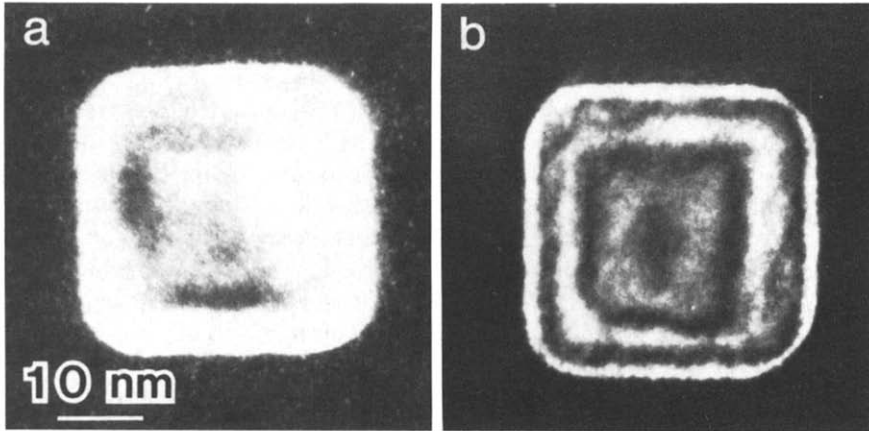


Fig. 8. Pair of dark field images of a square pyramidal particle using  $\pm(200)$  spots. For the strong beam condition of (a), large intensity variations corresponding to trace strains are present, which are not apparent in the medium beam image (b).

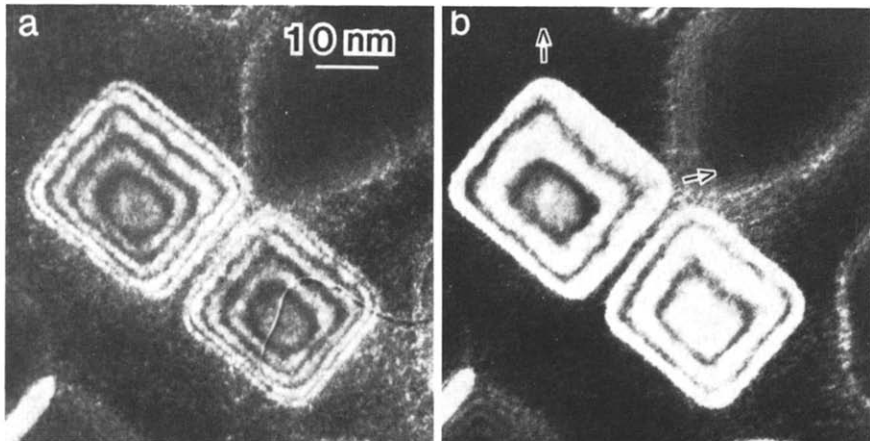


Fig. 9. Pair of  $\pm(200)$  dark field images of a single crystal. Comparing the fairly weak image in (a) to the medium beam images in (b), the contours in the medium beam image are distorted towards the corners as arrowed. This shows how strain effects distort medium beam images away from a valid representation of the 3D structure.

changes in intensity in dark field micrographs from particle to particle, can be found in refs. [23,68–69] and are also evident in fig. 4. (The standard procedure of transferring small particle specimens onto carbon films can introduce rotations on the mRad scale, as previously described [29].) More compelling (at first sight) are the diffraction results of Schabes-Retchkiman et al. [11]. However, these data (and the work in refs. [73,74]) only show the *average* diffraction, and thus *do not* show any inhomogeneous strain effects – inhomogeneous strains will modify the diffuse scattering around the main diffraction spots. Since there is also substantial diffuse scattering from plasmons (e.g. refs. [75,76]), phonons (e.g. ref. [77]) and shape effects (e.g. ref. [36]), the inhomogeneous strain effects will be essentially unobservable.

Therefore the evidence for homogeneous distortions is not convincing. In contrast, the evidence for inhomogeneous strains is quite clearcut. Refs. [7–9,12,14–15,23,31–33,68–69] show the same characteristic strain contrast as that described herein. This is not an exhaustive list, but it does include refs. [12,14,15] where the authors favor homogeneous strains. In particular, Schabes-Retchkiman and Yacaman [12] show a micrograph of an icosahedral MTP (fig. 7 in their paper) which displays very strong strain contrast, comparable to that in fig. 7c herein. Dislocations [25,26,29], which correlate with inhomogeneous elasticity calculations [20,21,30], and microdiffraction maps [29] also clearly indicate inhomogeneous strains. (Microdiffraction with a small beam as in ref. [29] shows the local fcc structure.)

There would also appear to be no evidence for large differences due to specimen preparation. We have referred herein to dark field evidence from many different authors, and the evidence for dislocations in ref. [29] was from a number of different specimens. We note that fig. 6 demonstrates that strain is present even in the smaller MTPs. It is also difficult to believe that coalescence of particles is relevant since this is a basic process in particulate growth (e.g. ref. [78]). The partially coalesced particles detailed in ref. [27] were originally hypothesised by Ino and Ogawa [8] and Komoda [18], although neither of these authors had adequate information for a concrete identification, whilst coalescence effects have been observed for MTPs in-situ by Yagi et al. [24]. We note the importance of Yagi et al.'s [24] results as the only unambiguous evidence of a true thermodynamic stability for MTPs (see also ref. [79]).

The question of which is correct, i.e. homogeneous or inhomogeneous strains, is only really critical for an energy calculation for small particles. If the particles are distorted fcc, homogeneous strains are not favored [30] since they leave unbalanced forces in the particles unless there is a Peierls distortion, concerning which some theoretical input would be useful. Until some strong theoretical reasons arise, we would rather not reject elasticity. Hence Occam's razor dictates that the particles are inhomogeneously strained.

Finally, we turn to the question of lattice parameter changes in small particles (e.g. refs. [2–6,80–82]), and how this relates to the earlier results

showing inhomogeneous strains in all the small gold single crystal particles. As a rule, experiments for small supported particles have concluded that the particles contract. However, it has recently become apparent that *clean* gold surfaces expand [70,71,83], an effect which can be linked to MTP formation [66,83,84]. Gold covered in carbon however shows perhaps a minimal contraction [70], an effect which can be attributed to the electronegative nature of the support [84,85] or interfacial stresses at the carbon-gold interface. It is important to consider this type of interfacial stress if we want to determine the source of the inhomogeneous strains in the single crystal particles. (We note that any source of stresses will generally lead to inhomogeneous strains.) Both the intrinsic stresses (surface stresses) at a free surface (e.g., ref. [2]), or interfacial stresses from surface impurities will give similar results, and we cannot with any confidence distinguish between them. This is true for essentially any experimental setup, in particular those of technological importance such as supported metal catalysts. Some clear-cut evidence for interfacial effects in small particles can be found in the paper by Heinemann et al. [1]. They found that small Pd particles on MgO grown and examined in UHV expand to relieve the epitaxial misfit, the expansion increasing with decreasing particle size (consistent with an elastic effect). Related work by Tholen [86,87] demonstrates that this type of contact strain is inhomogeneous. One must necessarily question the uniqueness of most of the evidence for contractions or expansions in small (hopefully single crystal) particle lattice parameters, particularly as most of the experiments have not even confirmed that single crystals were present. We can expect to find small particles inhomogeneously strained, but there are so many different possible sources that we cannot confidently discriminate between them.

Finally, we should consider the "theoretical evidence" for contractions in small particles (e.g. refs. [88-90]). Without doubting the utility of these analyses, we should be aware of the state-of-the-art. *Ab-initio* or even good approximate calculations with a reasonable number of atoms and the option of varying all atom co-ordinates independently to a minimum do not seem to be currently feasible. (An exception to this is the work of Farges et al. [28], which shows inhomogeneous strains.) The only variable available at present would appear to be a net volume change, thus including *only* homogeneous relaxations. We note that the homogeneous elasticity calculations of Ino [22] show a *contraction*, but inhomogeneous calculations [30] *do not*. (To be fair, Ino was only using homogeneous elasticity to approximate inhomogeneous elasticity.) Hence the contractions could be an artifact of the numerical approach. We also note that the expansion on gold depends upon a subtle electronic effect [71,84] which may provide difficult to accurately represent theoretically.

In conclusion, we find that there is no evidence for homogeneous strains in MTPs that cannot be ascribed to the first order (homogeneous) component of the inhomogeneous strain field in these particles. Unambiguous evidence from

dark field micrographs both herein and from earlier work by other authors says that these particles are inhomogeneously strained. This includes results by authors who have claimed no evidence for inhomogeneous strains. In the MTPs the strains are an intrinsic effect, but their source in single crystals cannot be uniquely determined. We also find that the source of lattice parameter changes in small particles does not have any simple and unique interpretation.

### Acknowledgements

The author would like to thank Drs. D.J. Smith and A. Howie for comments, advice and support during the course of the experimental work included in this paper, and Professor J.M. Cowley for useful comments. This work was supported on Department of Energy grant No. DE-AC02-76ER02995 and by the SERC, UK.

### References

- [1] K. Heinemann, T. Osaka, H. Poppa and M. Avalos-Borja, *J. Catalysis* 83 (1983) 61.
- [2] J.S. Vermaak, C.W. Mays and D. Kuhlmann-Wilsdorf, *Surface Sci.* 12 (1968) 128.
- [3] C.W. Mays, J.S. Vermaak and D. Kuhlmann-Wilsdorf, *Surface Sci.* 12 (1968) 134.
- [4] C. Solliard, *Surface Sci.* 106 (1981) 58.
- [5] M.A. Van Hove, R.J. Koestner, P.C. Stair, J.P. Biberian, L.L. Kesmodel, I. Bartos and G.A. Somorjai, *Surface Sci.* 103 (1981) 218.
- [6] J. Harada and K. Ohshima, *Surface Sci.* 106 (1981) 51.
- [7] S. Ino, *J. Phys. Soc. Japan* 21 (1966) 346.
- [8] S. Ino and T. Ogawa, *J. Phys. Soc. Japan* 22 (1967) 1369.
- [9] J.G. Allpress, and J.V. Sanders, *Surface Sci.* 7 (1967) 1.
- [10] B.G. Bagley, *Nature* 208 (1965) 674.
- [11] P. Schabes-Retchkiman, A. Gomez, G. Vazquez-Polo and M.J. Yacaman, *J. Vacuum Sci. Technol.* A2(1) (1984) 22.
- [12] P.S. Schabes-Retchkiman and M.J. Yacaman, *Appl. Surface Sci.* 11/12 (1982) 149.
- [13] M.J. Yacaman, in: *Catalytic Materials, Relationship Between Structure and Reactivity*, Eds. Whyte, Betta, Derouane and Baker (American Chemical Society, 1983) p. 341.
- [14] K. Heinemann, M.J. Yacaman, C.Y. Yang and H. Poppa, *J. Crystal Growth* 47 (1979) 187.
- [15] M.J. Yacaman, K. Heinemann, C.Y. Yang and H. Poppa, *J. Crystal Growth* 47 (1979) 177.
- [16] C.Y. Yang, *J. Crystal Growth* 47 (1979) 274.
- [17] C.Y. Yang, M.J. Yacaman and K. Heinemann, *J. Crystal Growth* 47 (1979) 283.
- [18] T. Komoda, *Japan. J. Appl. Phys.* 7 (1968) 27.
- [19] Y. Fukano and C.M. Wayman, *J. Appl. Phys.* 40 (1969) 1656.
- [20] R. de Wit, in: *Fundamental Aspects of Dislocation Theory*, Vol. 1, Eds. J.A. Simmons, R. de Wit and R. Bulbough, *Natl. Bur. Std. (US) Spec. Publ.* 317 (1969) 651, and, in particular, pp. 677–680.
- [21] R. de Wit, *J. Phys.* C5 (1972) 529.
- [22] S. Ino, *J. Phys. Soc. Japan* 27 (1969) 941.
- [23] S. Ogawa and S. Ino, in: *Advances in Epitaxy and Endotaxy*, Eds. Schneider and Ruth (Ottzlin Anderson Nexo., Leipzig) p. 183.

- [24] K. Yagi, K. Takayamagi, K. Kobayashi and G. Honjo, *J. Crystal Growth* 28 (1975) 117.
- [25] Y. Saito, S. Yatsuya, K. Mihama and R. Uyeda, *Japan. J. Appl. Phys.* 17 (1978) 1149.
- [26] L.D. Marks and D.J. Smith, *J. Crystal Growth* 54 (1981) 425.
- [27] D.J. Smith and L.D. Marks, *J. Crystal Growth* 54 (1981) 433.
- [28] J. Farges, M.F. de Feraudy, B. Raoult and J. Torchet, *Surface Sci.* 106 (1981) 95.
- [29] L.D. Marks and D.J. Smith, *J. Microscopy* 130 (1982) 249.
- [30] A. Howie and L.D. Marks, *Phil. Mag.* A49 (1984) 95.
- [31] K. Reichelt and H. Schreiber, *Surface Sci.* 43 (1974) 644.
- [32] K. Fukaya, S. Ino and S. Ogawa, *Trans. Japan. Inst. Metals* 19 (1978) 445.
- [33] T. Ohno and K. Yamauchi, *Japan. J. Appl. Phys.* 20 (1981) 1385.
- [34] M. Gillet, *Surface Sci.* 67 (1977) 139.
- [35] J. Buttet and J.P. Borel, *Helv. Phys. Acta* 56 (1983) 541.
- [36] P. Hirsch, A. Howie, R.B. Nicholson, D.W. Pashley and M.J. Whelan, in: *Electron Microscopy of Thin Crystals*, Huntington, NY, 1977, Ed. R.E. Krieger.
- [37] J.M. Cowley, *Diffraction Physics* (North-Holland, Amsterdam, 1981).
- [38] A.J.F. Metherell, in: *Electron Microscopy in Material Science*, Eds. U. Valdrè and E. Ruedl (Commission of the European Communities, 1975) Vol. II, p. 397.
- [39] C.J. Humphreys, *Rept. Progr. Phys.* 42 (1979) 122.
- [40] C.J. Humphreys, in: *Dislocations in Solids*, Ed. F.R.N. Nabarro (North-Holland, New York, 1980) Vol. 5, p. 1.
- [41] L. Reimer, *Transmission Electron Microscopy* (Springer, Berlin, 1984).
- [42] R.M. Stern, J.J. Perry and D.S. Boudreaux, *Rev. Mod. Phys.* 41 (1969) 275.
- [43] P.G. Self, M.A. O'Keefe, P.R. Buseck and A.E.C. Spargo, *Ultramicroscopy* 11 (1983) 35.
- [44] J.M. Cowley and A.L.G. Rees, *Proc. Phys. Soc. (London)* 59 (1947) 287.
- [45] L. Sturkey, *Phys. Rev.* 73 (1948) 183.
- [46] J.M. Cowley, P. Goodmann and A.L.G. Rees, *Acta Cryst.* 10 (1957) 19.
- [47] K. Moliere and H. Wagenfeld, *Z. Krist.* 110 (1958) 3.
- [48] G. Lempfuhl and A. Reissland, *Z. Naturforsch.* 23a (1968) 544.
- [49] N. Kato, *J. Phys. Soc. Japan*, 18 (1963) 1785.
- [50] L.D. Marks, *Acta Cryst.*, submitted.
- [51] M. Born and E. Wolf, *Principles of Optics* (Pergamon, London, 1959).
- [52] D.J.H. Cockayne, I.L.F. Ray and M.J. Whelan, *Phil. Mag.* 20 (1969) 1265.
- [53] D.J.H. Cockayne, *J. Microscopy* 98 (1973) 116.
- [54] W.M. Stobbs, in: *Electron Microscopy in Materials Science*, Eds. U. Valdrè and E. Ruedl (Commission of the European Communities, 1975) Vol. II.
- [55] T. Katagawa and N. Kato, *Acta Cryst.* A30 (1974) 830.
- [56] O. Litzman and Z. Janacek, *Phys. Status Solidi* 25 (1974) 663.
- [57] P.V. Petrashen and F.N. Chukhovskii, *Soviet Phys.-JETP* 69 (1975) 477.
- [58] Z.G. Pinsker, *Dynamical Scattering of X-Rays in Crystals* (Springer, New York, 1978).
- [59] S. Takagi, *Acta Cryst.* 15 (1962) 1311.
- [60] H. Hashimoto and M. Mannami, *Acta Cryst.* 13 (1960) 363.
- [61] A. Howie and Z.S. Basinski, *Phil. Mag.* 17 (1968) 1039.
- [62] B. Jouffrey and D. Taupin, *Phil. Mag.* 16 (1967) 703.
- [63] A. Howie and C.H. Sworn, *Phil. Mag.* 22 (1970) 861.
- [64] A.K. Head, P. Humble, L.M. Clarebrugh, A.J. Morton and C.T. Forwood, *Computer Electron Micrographs and Defect Identification* (North-Holland, Amsterdam, 1973).
- [65] B. Moss and D.L. Dorset, *Acta Cryst.* A39 (1983) 609.
- [66] C. Kittel, *Quantum Theory of Solids* (Wiley, New York, 1963).
- [67] N. Kato, in: *Characterization of Crystal Growth Defects by X-Ray Methods*, Eds. B.K. Tanner and D.K. Bowen (Plenum, New York, 1980) p. 264.
- [68] K. Heinemann, M. Avalos-Borja and H. Poppa, *Inst. Phys. Conf. Ser.* 52, ch. 8 (1980) 387.

- [69] D.A. Smith and M.M.J. Treacy, *Appl. Surface Sci.* 11/12 (1982) 131.
- [70] L.D. Marks, *Phys. Rev. Letters* 51 (1983) 1000.
- [71] L.D. Marks, V. Heine and D.J. Smith, *Phys. Rev. Letters* 52 (1984) 656.
- [72] L.D. Marks, *Surface Sci.* 139 (1984) 281.
- [73] S. Matsumoto and Y. Matsui, *J. Mater. Sci.* 18 (1983) 1785.
- [74] R.A. Roy, J. Messier and J.M. Cowley, *Thin Solid Films* 79 (1981) 207.
- [75] A. Howie, *Proc. Roy. Soc. (London)* A271 (1963) 268.
- [76] H. Reather, *Excitation of Plasmons and Interband Transitions by Electrons* (Springer, Berlin, 1980).
- [77] P. Rez, C.J. Humphreys and M.J. Whelan, *Phil. Mag.* 35 (1977) 81.
- [78] D.W. Pashley and M.J. Stowell, *J. Vacuum Sci. Technol.* 3 (1966) 156.
- [79] L.D. Marks, *J. Crystal Growth* 61 (1983) 556.
- [80] H.J. Wasserman and J.S. Vermaak, *Surface Sci.* 32 (1972) 168.
- [81] G. Apai, J.F. Hamilton, J. Stohr and A. Thompson, *Phys. Rev. Letters* 43 (1979) 165.
- [82] B. Moraweck and A.J. Renouprez, *Surface Sci.* 106 (1981) 35.
- [83] L.D. Marks and D.J. Smith, *Surface Sci.* 143 (1984) 495.
- [84] V. Heine and L.D. Marks, in preparation.
- [85] L.D. Marks and V. Heine, *J. Catalysis*, submitted.
- [86] A.R. Tholen, *Acta Met.* 27 (1979) 1765.
- [87] A.R. Tholen, *Microscopic Aspects of Adhesion and Lubrication* (Elsevier, Amsterdam, 1982) p. 263.
- [88] J.G. Allpress and J.V. Sanders, *Australian J. Phys.* 23 (1970) 23.
- [89] M.B. Gordon, F. Cyrot-Lackmann and M.C. Desjonquères, *Surface Sci.* 80 (1979) 159.
- [90] J.L. Martins, R. Carr and J. Buttet, *Surface Sci.* 106 (1981) 265.